Title

Asymmetric responses of Land Hydroclimatology to Two types of El Niño in the Mississippi River Basin

Journal
Geophysical Research Letters, 41(2)

ISSN
00948276

Authors
Liang, Yu-Chiao
Lo, Min-Hui
Yu, Jin-Yi

Publication Date
2014

DOI
10.1002/2013GL058828

AGU PUBLICATIONS

Geophysical Research Letters

RESEARCH LETTER
10.1002/2013GL058828

Key Points:
- CP and EP El Nino have opposite effects on water cycle in the Mississippi River
- Subsurface water is essential to extend El Nino impact from winter to spring
- If CP El Nino becomes prevailing, potential exists of frequent water shortages

Correspondence to:
M.-H. Lo,
minhuilo@ntu.edu.tw

Citation:
Liang, Y.-C., M.-H. Lo, and J.-Y. Yu (2014), Asymmetric responses of land hydroclimatology to two types of El Niño in the Mississippi River Basin, *Geophys. Res. Lett.*, *41*, 582–588, doi:10.1002/2013GL058828.

Received 25 NOV 2013
Accepted 3 JAN 2014
Accepted article online 6 JAN 2014
Published online 28 JAN 2014

Asymmetric responses of land hydroclimatology to two types of El Niño in the Mississippi River Basin

Yu-Chiao Liang[1,2], Min-Hui Lo[1], and Jin-Yi Yu[2]

[1]Department of Atmospheric Sciences, National Taiwan University, Taipei, Taiwan, [2]Department of Earth System Science, University of California-Irvine, Irvine, California, USA

Abstract El Niño events play important roles in influencing the hydroclimatology over the Mississippi River Basin (MRB). This study shows that the two types of El Niño events, the central Pacific (CP) El Niño and eastern Pacific (EP) El Niño, have opposite effects on spring soil water hydrology in the MRB. Above-normal spring (March) precipitation during EP El Niño years leads to higher soil water levels during the subsequent 2 to 3 months in the central and western MRB. On the other hand, CP El Niño events induce below-normal spring precipitation that causes lower soil water levels over the Ohio-Mississippi Valley during the following 1 or 2 months. As a result, a springtime asymmetric response occurs in the MRB streamflow and soil water storage to the two types of El Niño. Subsurface hydrological storage processes are found to be essential to extend El Niño's influence in the MRB to late spring.

1. Introduction

The Mississippi River Basin (MRB) is the largest drainage basin in North America, covering an area of approximately 3.2×10^6 km^2 to about 41% of the contiguous United States. The freshwater resources in the MRB support the extensive agricultural activity in the Central United States. Therefore, it is important to understand surface and groundwater hydrology in the MRB and how they respond to climate variation and change [*Goolsby et al.*, 1999]. The El Niño–Southern Oscillation (ENSO) can significantly influence temperature and precipitation throughout the U.S. [e.g., *Ropelewski and Halpert*, 1986; *Rogers and Coleman*, 2004; *Kurtzman and Scanlon*, 2007], including the MRB. Previous observational and modeling studies [e.g., *Kahya and Dracup*, 1993; *Twine et al.*, 2005; *Dai et al.*, 2009] found a close connection between ENSO and MRB streamflow. *Twine et al.* [2005], for example, analyzed model simulations and observational data to show that ENSO events increase spring streamflow in MRB. *Dai et al.* [2009] explored a long-term river flow data set and confirmed that El Niño events tend to enhance the Mississippi River streamflow.

ENSO-induced precipitation anomalies can affect the storage of water in soil and groundwater, which can significantly influence hydrological processes in the MRB. Based on the available global soil moisture data set, *Entin et al.* [2000] found a lag of 2 to 3 months in soil moisture storage in response to the precipitation anomalies. *Chen and Kumar* [2002] further illustrated the relationship between ENSO and hydrological variables, including soil water storage and river streamflow. Using a modeling approach, *Lo and Famiglietti* [2010] demonstrated that subsurface hydrological processes can affect the timing of soil moisture storage, and therefore, play important roles in preserving the precipitation signals in terrestrial water (soil and groundwater) storage and influencing streamflow in the subsequent months or seasons in the MRB.

Recently, it was suggested that there are two types of ENSO—an eastern Pacific (EP) El Niño and a central Pacific (CP) El Niño [e.g., *Yu and Kao*, 2007; *Ashok et al.*, 2007; *Kao and Yu*, 2009; *Kug et al.*, 2009]. The EP El Niño is characterized by positive sea surface temperature (SST) anomalies extending from the South American coast westward along the equator. However, positive SST anomalies can also evolve mostly in the central Pacific around the international dateline forming the CP El Niño [*Kao and Yu*, 2009]. The formation and mechanism of CP and EP El Niño have been evaluated by examining two empirical orthogonal function (an analytical technique based on eigenvalue decomposition to identify characteristic patterns of physical fields) patterns of SST anomalies in the tropical Pacific [*Ashok et al.*, 2007; *Kao and Yu*, 2009; *Kug et al.*, 2009]. These two types of ENSO can lead to different convection patterns and atmospheric responses [*Mo*, 2010; *Yu et al.*, 2012a; *Yu and Zou*, 2013], resulting in distinct impacts on regional and global climate [*Li et al.*, 2011; *Karori et al.*, 2013]. Over the United States, for example, CP

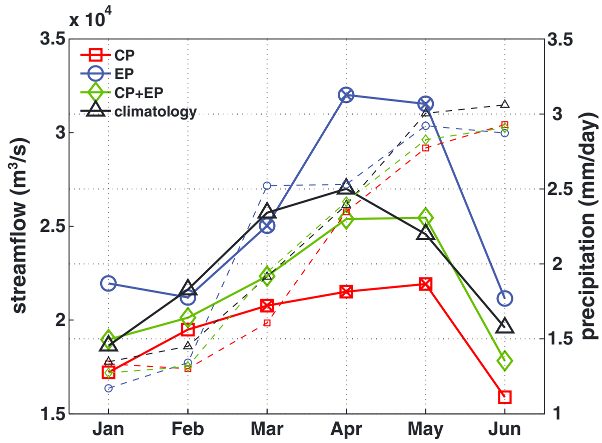

Figure 1. Monthly Mississippi River streamflow gauged at Vicksburg, USA. The climatology streamflows calculated from 1950 to 2006 are shown by the black line, while the streamflows are shown in red for the CP El Niño composite, in blue for the EP El Niño composite, and in green for the all-El Niño composite. The "cross" indicates that the difference in streamflow between the CP and EP El Niño composites is statistically significant. The dashed lines show area-averaged precipitation in MRB.

El Niño events cause negative precipitation anomalies along the Ohio-Mississippi Valley during late winter, while EP El Niño events produce wet anomalies in the central U.S. as shown in *Mo* [2010] and *Yu and Zou* [2013].

Although previous studies have looked into the relationship between hydrological processes and ENSO, few studies have considered El Niño's effects on soil water storage and streamflow for the CP and EP El Niño types separately. Because the location of El Niño has shifted more from the EP to the CP during the recent few decades [*Ashok et al*., 2007; *Kug et al*., 2009; *Yu et al*., 2012b], it is necessary to ascertain whether these two types of El Niño produce different impacts on the streamflow and soil water storage in the MRB.

2. Data and Methods

The Global River Flow and Continental Discharge Data Set from *Dai et al*. [2009] was used for analysis in this study, which includes the 1900–2006 monthly streamflow for the Mississippi River at the most downstream gauging station (Vicksburg, Mississippi) and the simulated streamflow from the National Center for Atmospheric Research Community Land Model. To examine the processes responsible for the variations in streamflow and their relationships with atmospheric forcing, monthly soil moisture and precipitation (including rainfall and snowfall) from 1950 to 2006 were obtained from Global Land Data Assimilation System version 2 (GLDAS2) data set [*Rodell et al*., 2004]. The atmospheric forcings in GLDAS2 are based on *Sheffield et al*. [2006]. There are four soil layers in the GLDAS2 data set with the lower boundaries at 10 cm, 50 cm, 100 cm, and 200 cm, respectively. In this study, anomalies are defined as the deviations from the 1950–2006 climatology, and the statistical significance of the anomalies was evaluated using Student's *t* tests with a 90% significance level.

There are several different identification methods to determine whether an El Niño event is of the EP type or the CP type. *Yu et al*. [2012a] combined three different methods to define a "consensus El Niño type" for the major El Niño events occurring after 1950. These methods are the EP/CP-index method from *Kao and Yu* [2009], the Niño3 versus Niño4 method from *Yeh et al*. [2009], and the El Niño Modoki method from *Ashok et al*. [2007]. During our analysis period, seven EP El Niño events (1951–1952, 1969–1970, 1972–1973, 1976–1977, 1982–1983, 1986–1987, and 1997–1998) and 12 CP El Niño events (1953–1954, 1957–1958, 1958–1959, 1963–1964, 1965–1966, 1968–1969, 1977–1978, 1987–1988, 1991–1992, 1994–1995, 2002–2003, and 2004–2005) were identified for analyses.

3. Results

3.1. Asymmetric Responses of Mississippi River Streamflow

We first examined Mississippi River streamflow (at Vicksburg, Mississippi) using the global streamflow data set from *Dai et al*. [2009]. The monthly streamflow from January to June after El Niño events reach their peak intensities were composited based on the seven EP El Niño and 12 CP El Niño events. The composites are shown and compared in Figure 1 with the streamflow climatology. Figure 1 shows that the streamflow climatology (black solid) increases from January, reaches its peak in April, and then gradually declines. During the EP El Niño (blue solid), the MRB streamflow is significant above normal after March. During the CP El Niño (red solid), the streamflow is below normal throughout January to June, and the largest difference occurs in April, about 20% less than the climatological volume. In contrast, the largest difference during the EP El Niño occurs in May, about 28% more than the climatological value. These two types of El Niño cause the MRB

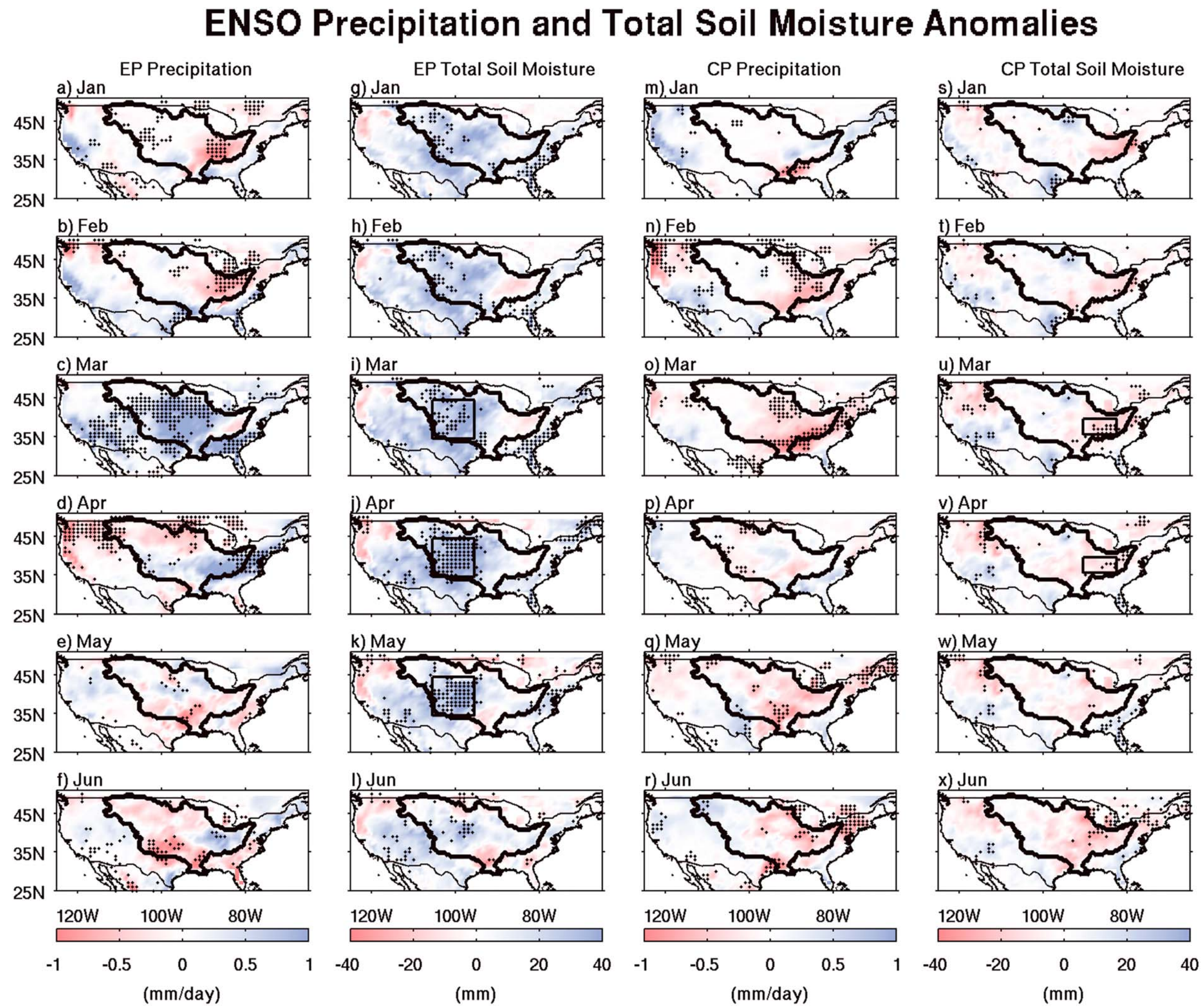

Figure 2. January to June precipitation (millimeter/day) and total soil moisture (millimeter) anomalies during the EP and CP El Niño. The two left columns show the composited for the CP El Niño events (for (a–f) precipitation anomalies and for (g–l) total soil moisture anomalies), and the two right columns show the composite for the CP El Niño (for (m–r) precipitation anomalies and for (s–x) total soil moisture anomalies). Statistically, significant results are dotted. The thick black line delineates the boundary of MRB. The rectangular boxes in Figures 2i–2k cover 95°–105°W and 34°–45°N, while the ones in Figures 2u–2v cover 80°–90°W and 35°–40°N.

streamflow to fluctuate in a range of about half of the climatological streamflow amount, which is profound. If the El Niño impact is not stratified according to the El Niño type, the streamflow composite for all the 19 El Niño events is near or moderately below normal (see the green solid line in Figure 1). This pattern differs from findings from previous studies [e.g., *Twine et al.*, 2005] and most likely results from the calculation method used here which includes more CP El Niño events occurring in the recent decades.

Figure 1 shows the negative streamflow anomalies produced by the all-El Niño composite are at most only half of the anomalies produced by the CP El Niño. The analysis shown in Figure 1 indicates that a stronger and clearer impact of El Niño on the MRB streamflow can be demonstrated when the El Niño type is considered. Also, the difference in streamflow between the two types of El Niño are found to be most statistically significant in March, April, and May, indicating that the two types of El Niño produce the most different impacts on the springtime MRB streamflow. Note that we also compared the MRB streamflow during the developing phase of El Niño but found no significant difference between the CP and EP El Niño (not shown).

The asymmetric response of the streamflow between the CP and EP El Niño years is likely to be related to the patterns of precipitation and the evolution of total soil water storage in the MRB. The area-averaged precipitations (dashed lines in Figure 1) have revealed the linkage between precipitation and streamflow in the MRB, in which, the most significant change in precipitation is in March, and the most significant change in streamflow is

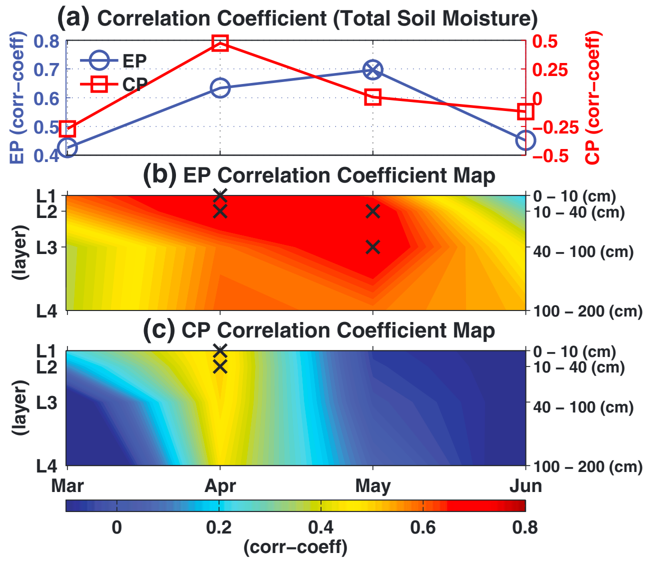

Figure 3. (a) Correlation coefficients between March precipitation anomalies and total soil moisture anomalies in the subsequent months calculated from the CP El Niño composite (red squares with respect to right, red *y* axis) and the EP El Niño composite (blue circles with respect to left, blue *y* axis). Correlation coefficients between March precipitation anomaly and soil moisture anomalies in different layers are shown in (b) the EP El Niño composite and in (c) the CP El Niño composite. The regions chosen for all these calculations are shown in Figure 2i for the EP El Niño and in Figure 2u for the CP El Niño. The symbol "cross" shown in Figures 3a, 3b, and 3c denotes the significant point with *p* value less than 0.1.

in April and May. To understand how the asymmetric streamflow responses are produced, we examined in Figure 2 the evolution of the monthly precipitation and total soil moisture anomalies from GLDAS2 data set. In the figure, the regions where the anomalies are 90% statistically significant are dotted. Similar results (not shown) were obtained when the analysis was repeated with another precipitation data from the Parameter-elevation Regressions on Independent Slopes Model [http://prism.oregonstate.edu]. The strongest precipitation anomalies in the MRB were observed in early spring (March through April), when above-normal precipitations first prevail over most of the central MRB and then move to eastern MRB. In late winter (January and February), negative precipitation anomalies were observed over the Ohio-Mississippi Valley and in late spring and earlier summer (May and June) over the southern MRB, but their magnitudes are relatively small and confined to specific areas.

When EP El Niño occurs, the total soil moisture (sum of the four soil layers above 200 cm depth) anomalies show an overall wetness in the MRB from January to June (Figures 2g–2l). The wet soil anomalies in January and February are in fact associated with the positive precipitation anomalies that occur during the late autumn and earlier winter of the previous year (i.e., the developing phase of El Niño; results not shown). The largest soil moisture anomalies were observed in the western MRB from March to May, which occur up to 2 months after the largest precipitation anomalies were produced in the region. Wet soil anomalies actually can still be found in the MRB until June. The evolution of precipitation in Figures 2a–2f and soil moisture in Figures 2g–2l indicate that there is a 2 to 3 month lag in total soil moisture response to the above-normal precipitation anomalies induced by the EP El Niño in the MRB.

During the CP El Niño, a different picture emerges when we examined the evolution of precipitation and soil moisture anomalies. First of all, negative precipitation anomalies (Figures 2m–2r) persist throughout January to June in the MRB. The negative anomalies have the largest magnitudes from February to March, which is consistent with the finding of *Yu and Zou* [2013] that the CP El Niño produces a stronger winter drying effect over the Ohio-Mississippi River valley than the EP El Niño does. They attributed this enhanced drying effect of the CP El Niño to the more southward displacement of the tropospheric jet streams that steer the movements of winter storm over the United States. The second difference appears in the lagged response of the total soil moisture to the precipitation anomalies. As can be seen from Figures 2s–2x, below-normal soil moisture were accumulated in the MRB during the CP El Niño, which is expected from the below normal precipitation induced by the CP El Niño. Besides, a shorter lag relationship between the soil moisture anomalies and the precipitation anomalies was observed, reflecting the weaker precipitation anomalies in magnitude during the CP El Niño. Statistically, significant dry soil moisture anomalies in the MRB were observed only in March and April, despite the relative large negative precipitation anomalies in February and March. Apparently in the MRB, dry precipitation anomalies have a less-persistent impact on soil moisture than the impact produced by the wet precipitation anomalies during the EP El Niño.

3.2. Subsurface Hydrological Processes

To further illustrate the relationship between precipitation anomalies in March and total soil water storage in the subsequent months, we compared the correlation between the March precipitation anomalies and the total soil

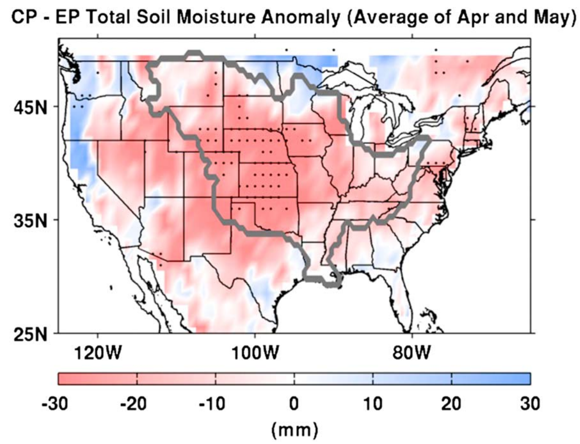

Figure 4. Difference in total soil moisture (averaged from April to May) between CP El Niño and EP El Niño. Statistically significant results are dotted.

moisture anomalies from March to June. The correlation was calculated in a rectangular box in 95°–105°W and 34°–45°N for the EP El Niño composite and a box in 80°–90°W and 35°–40°N for CP El Niño composite as indicated in Figures 2i and 2u, respectively. As shown in Figure 3a, the correlation coefficient for the EP El Niño composite increases from March to May, implying that the water from the intense positive precipitation anomalies in March is stored and accumulated in the central and western MRB, corresponding to the lag response of total soil water storage shown in Figure 2. On the other hand, the positive correlation coefficients for the CP El Niño composite only increase from March to April, reflecting a lag of about 1 month after the maximum negative precipitation anomaly occurs in March. In other months the correlation becomes weaker, implying fewer impacts from the weak negative precipitation anomalies during CP El Niño.

In addition to the total soil moisture, we also considered at which soil depths the precipitation anomalies can impact the soil moisture. Figure 3b shows the correlation coefficients between the March precipitation anomalies and soil moisture anomalies at different soil layer depths during the EP El Niño. The figure indicates that the positive precipitation anomaly in March penetrates to the surface soil layers in April, including layer L1 (0–10 cm) and L2 (10–40 cm). In May, the influence of precipitation anomalies is no longer confined to surface soil layers but reaches layer L4 (100–200 cm). Deep soil layers are known to play an important role in producing lagged responses to atmospheric forcing, which significantly affects the slow response component of streamflow (or groundwater flow) [e.g., *Niu et al.*, 2005; *Yeh and Eltahir*, 2005; *Lo et al.*, 2008]. The vertical penetration of water in the soil can be viewed as a transport of precipitation signals from surface to deeper layers, showing the restoration of ENSO signals in the land memory effect. Similar vertical propagation of soil water can be seen in CP El Niño in Figure 3c, but the signal cannot persist longer than 1 month because of the weaker negative precipitation anomalies. Also, the dry precipitation anomalies can only penetrate to the layer of L2 during the CP El Niño.

Our analyses of the soil moisture storage explain why the MRB streamflow responds differently to the two types of El Niño. During EP El Niño events, positive precipitation anomalies in early spring can penetrate to a deep layer of soil to enhance soil water storage in April and May over the central and western MRB. This 2 to 3 months lagged increase in the total soil water storage is then reflected as an increase in the MRB streamflow. On the other hand, CP El Niño events cause negative precipitation anomalies that penetrate only to a shallower layer of soil in the eastern portion of MRB with a shorter lag of 1–2 months. The decreased content in the total soil water storage then leads to reduced streamflow rate in the subsequent 1–2 months. Evaporation and the snow melt can also contribute to changes in streamflow when CP and EP El Niño events occur. However, the region of significant snow melt in the U.S. occurs outside the northern MRB, and the evaporation is relatively small during the spring season; hence, they have limited effects on the results shown here.

4. Discussion

Chou and Lo [2007] showed that the El Niño and La Niña can cause asymmetric responses of tropical precipitation along the equator. The current study further shows that even in the same warm phase of ENSO, changes in the location of El Niño can cause significantly different responses in soil water storage and streamflow in the MRB. *Eltahir and Yeh* [1999] discussed the nonlinear behavior of groundwater discharge on aquifers water level, which can explain the mechanism of soil water restoration. Without land subsurface hydrological storage, the impacts of EP/CP El Niño cannot persist from earlier spring (or late winter), when El Niño events typically peak and their impacts on the U.S. are the strongest, to the subsequent seasons. These findings indicate that including the role of the memory of subsurface land hydrological processes in future empirical or numerical modeling studies [e.g., *Lo and Famiglietti*, 2011] will be necessary to better explore the relationships analyzed here.

The location of El Niño has gradually shifted from the eastern Pacific to the central Pacific during the recent two decades. *Yu and Zou* [2013] already showed that the altered atmospheric circulation tends to enhance negative precipitation anomalies in the MRB when CP El Niño occurs. Our study further indicates that the negative precipitation anomalies can decrease the total soil water content in the western MRB (Figure 4), which can lead to a reduced river streamflow in the Mississippi River. Consistent results were also found in offline simulations with the Community Land Model version 4 using the same GLDAS2 atmospheric forcings, indicating that our results are model-independent. Although in general, the strength of CP El Niño is not as strong as that of EP El Niño, the overall drier land conditions and reduced river streamflow could pose water shortages or severe drought and threaten agricultural water supplies in the central United States.

Acknowledgments
The GLDAS data set is from http://grace.jpl.nasa.gov, which used the Goddard Earth Sciences Data and Information Services Center. This work was supported by the National Science Council grant 102-2111-M-002-003 to National Taiwan University, National Science Council grant NSC-100-2119-M-001-029-MY5, NTU-CESRP-102R7604-1 from the National Taiwan University, and Taida Institute for Mathematical Sciences for the additional support. Jin-Yi Yu was supported by NOAA-MAPP grant NA11OAR4310102 and NSF grant AGS-1233542.

The Editor thanks two anonymous reviewers for their assistance in evaluating this paper.

References

Ashok, K., S. K. Behera, S. A. Rao, H. Weng, and T. Yamagata (2007), El Niño Modoki and its possible teleconnection, *J. Geophys. Res.*, *112*, C11007, doi:10.1029/2006JC003798.

Chen, J., and P. Kumar (2002), Role of terrestrial hydrologic memory in modulating ENSO impacts in North America, *J. Clim.*, *15*, 3569–3585.

Chou, C., and M.-H. Lo (2007), Asymmetric responses of tropical precipitation during ENSO, *J. Clim.*, *19*, 3411–3433.

Dai, A., T. Qian, and K. E. Trenberth (2009), Changes in continental freshwater discharge from 1948 to 2004, *J. Clim.*, *22*, 2773–2792.

Eltahir, E. A. B., and P. J. F. Yeh (1999), On the asymmetric response of aquifer water level to floods and droughts in Illinois, *Water Resour. Res.*, *35*(4), 1199–1217.

Entin, J. K., A. Robock, K. Y. Vinnikov, S. E. Hollinger, S. Liu, and A. Namkhai (2000), Temporal and spatial scales of observed soil moisture variations in the extratropics, *J. Geophys. Res.*, *105*, 11,865–11,877.

Goolsby, D. A., et al. (1999), Flux and sources of nutrients in the Mississippi-Atchafalaya River basin: Topic 3 Report for the Integrated Assessment if Hypoxia in the Gulf of Mexica. NOAA Coastal Ocean Office, Series No. 17.

Kahya, E., and J. A. Dracup (1993), U.S. streamflow patterns in relation to the El Niño/Southern Oscillation, *Water Resour. Res.*, *42*, 2491–2503.

Kao, H.-Y., and J.-Y. Yu (2009), Constrasting eastern-Pacific and central-Pacific types of ENSO, *J. Clim.*, *22*, 615–632, doi:10.1175/2008JCLI2309.1.

Karori, M. A., J. Li, and F.-F. Jin (2013), The asymmetric influence of the two types of El Niño and La Nina on summer rainfall over southeast China, *J. Clim.*, *26*, 4567–4582.

Kug, J.-S., F.-F. Jin, and S.-I. An (2009), Two types of El Niño events: Cold Tongue El Niño and Warm Pool El Niño, *J. Clim.*, *22*, 1499–1515, doi:10.1175/2008JCLI2624.1.

Kurtzman, D., and B. R. Scanlon (2007), El Niño-Southern Oscillation and Pacific Decadal Oscillation impacts on precipitation in the southern and central United States: Evaluation of spatial distribution and predictions, *Water Resour. Res.*, *43*, W10427, doi:10.1029/2007WR005863.

Li, W., P. Zhang, J. Ye, L. Li, and P. A. Baker (2011), Impact of two different types of El Niño events on the Amazon climate and ecosystem productivity, *J. Plant Ecol.*, *4*, 91–99, doi:10.1093/jpe/rtq039.

Lo, M.-H., and J. S. Famiglietti (2010), The effect of water table dynamics on land surface hydrologic memory, *J. Geophys. Res.*, *115*, D22118, doi:10.1029/2010JD014191.

Lo, M.-H., and J. S. Famiglietti (2011), Precipitation response to land subsurface hydrologic processes in atmospheric general circulation model simulations, *J. Geophys. Res.*, *116*, D05107, doi:10.1029/2010JD015134.

Lo, M.-H., P. J.-F. Yeh, and J. S. Famiglietti (2008), Using baseflow to constrain water table depth simulations in the NCAR Community Land Model (CLM), *Adv. Water Resour.*, *31*(12), 1552–1564, doi:10.1016/j.advwatres.2008.06.007.

Mo, K. C. (2010), Interdecadal modulation of the impact of ENSO on precipitation and temperature over the United States, *J. Clim.*, *23*, 3639–3656, doi:10.1175/2010JCLI3553.1.

Niu, G.-Y., Z.-L. Yang, R. E. Dickinson, and L. E. Gulden (2005), A simple TOPMODEL-based runoff parameterization (SIMTOP) for use in GCMs, *J. Geophys. Res.*, *110*, D21106, doi:10.1029/2005JD006111.

Rodell, M., et al. (2004), The Global Land Data Assimilation System, *Bull. Am. Meteorol. Soc.*, *85*, 381–394, doi:10.1175/BAMS-85-3-381.

Rogers, J. C., and J. S. M. Coleman (2004), Ohio winter precipitation and stream flow associations to Pacific atmospheric and oceanic teleconnection patterns, *Ohio J. Sci.*, *104*(3), 51–59.

Ropelewski, C. F., and M. S. Halpert (1986), North America precipitation and temperature patterns associated with the El Niño/Southern Oscillation (ENSO), *Mon. Weather Rev.*, *114*, 2352–2362.

Sheffield, J., G. Goteti, and E. F. Wood (2006), Development of a 50-yr high-resolution global dataset of meteorological forcings for land surface modeling, *J. Clim.*, *19*(13), 3088–3111.

Twine, T. E., C. J. Kucharik, and J. A. Foley (2005), Effects of El Niño-Southern Oscillation on the climate, water balance, and streamflow of the Mississippi River Basin, *J. Clim.*, *18*, 4840–4861.

Yeh, P. J.-F., and E. A. B. Eltahir (2005), Representation of water table dynamics in a land surface scheme. Part I: Model development, *J. Clim.*, *18*, 1861–1880.

Yeh, S.-W., J.-S. Kug, B. Dewitte, M.-H. Kwon, B. P. Kirtman, and F.-F. Jin (2009), El Niño in a changing climate, *Nature*, *461*, 511–514, doi:10.1038/nature08316.

Yu, J.-Y., and H.-Y. Kao (2007), Decadal changes of ENSO persistence barrier in SST and ocean heat content indices: 1958–2001, *J. Geophys. Res.*, *112*, D13106, doi:10.1029/2006JD007654.

Yu, J.-Y., and Y. Zou (2013), The enhanced drying effect of central-Pacific El Niño on US winter, *Environ. Res. Lett.*, *8*, 014019, doi:10.1088/1748-92326/8/1/014019.

Yu, J.-Y., Y. Zou, S. T. Kim, and T. Lee (2012a), The changing impact of El Niño on US winter temperatures, *Geophys. Res. Lett.*, *39*, L15702, doi:10.1029/2012GL052483.

Yu, J.-Y., M.-M. Lu, and S. T. Kim (2012b), A change in the relationship between tropical central Pacific SST variability and the extratropical atmosphere around 1990, *Environ. Res. Lett.*, *7*, 034025, doi:10.1088/1748-9326/7/3/034025.

